ELSEVIER

Polymer 43 (2002) 395–401

polymer

www.elsevier.com/locate/polymer

Mesoscopic simulation of dynamic crack propagation in rubber materials ☆

G. Heinrich[a,*], J. Struve[a], G. Gerber[b]

[a]*Tire Research/Materials Research, Continental Aktiengesellschaft, Strategic Technology, P.O. Box 169, D-30001 Hannover, Germany*
[b]*ISMANS, avenue F.A. Bartholdi 44, F-72000 Le Mans, France*

Abstract

Tear fatigue analyzer (TFA) tests on rubber are simulated, for the first time, with a combination of a mesoscopic model of self-similar crack propagation and a complex viscoelastic rubber model (flow-enhanced linear standard solid). In this way, it is possible to establish interconnections between mechanical fracturing tests (TFA) and intrinsic material properties. © 2001 Elsevier Science Ltd. All rights reserved.

Keywords: Rubber materials; Crack propagation; Tear fatigue analyzer tests

1. Introduction

Service life prediction of materials is clearly of high practical and scientific interest and has attracted the attention of chemists, engineers, and physicists [1]. In the case of rubber and other polymer materials, it is reasonable to assume that microcracks from which failure originates are formed via the sequence of several steps [2]: (i) molecular chains attempt to move in tensile direction, causing a slip between chains and producing reorientation; (ii) cross-links, entanglements and filler particles hinder the motion of chains. Chains acquire a state of tension and local scission occurs; (iii) scission of one chain transfers stress to the neighboring chains, chain scission propagates to the surrounding molecules; the cumulative effect produces a microvoid; (iv) microvoids that have grown to a critical size, say c_0, form microcracks which continue to grow irreversibly.

However, estimating the fatigue lifetime of elastomeric components is still a difficult task for compound chemists and designers in rubber industry. Even an FE optimized design according to stress, strain or even energy based parameters can lead to unexpected failure in service, sometimes in component areas expected as low loaded. Therefore, it is essential to use fracture mechanics methods to characterize the toughness of different elastomers under quasi-static and dynamic stress when predicting the life of highly stressed elastomer components. Using these methods — with only moderate test expenditure — leads to optimization strategies for new applications [3–10].

However, the application of fracture mechanics to rubber generates some difficulties because of the large deformation of elastomers. In particular, elasticity of rubbers is not linear, and, more over, highly deformed cracks do not stay sharp as in the Griffith's model (A. A. Griffith, Philosoph Trans R Soc Lond A221 (1920) 163; see, for example Ref. [11]). Nevertheless, a step forward in life estimation is fracture mechanics-based parameters which include the material's susceptibility against crack initiation, and the toughness of the material against crack propagation. These mostly energy-based parameters like tearing energy or J-integral regard the necessary loading for crack propagation at different crack propagation velocities. This allows ranking different materials under the same loading conditions. Nevertheless, there are several fundamental issues unsolved in the fracture mechanics of rubber-like solids.

For the quasi-static load case, the material behavior of a pre-damaged sample, under increasing load, is compared with a pre-determined damage parameter. The material analysis is conducted according to tension, deformation, or energy variables under specific damage propagation, e.g. with technically recordable crack initiation and maximum crack length before a sample breaks (see also e.g. Refs. [3–7]).

For the dynamic load case, the damage progress is first determined over the period of a pre-cracked sample with fixed stress parameters (e.g. with TFA tests [5]; see

☆ This paper was originally submitted to *Computational and Theoretical Polymer Science* and received on 23 March 2001; received in revised form on 26 June 2001; accepted on 28 June 2001. Following the incorporation of *Computational and Theoretical Polymer Science* into *Polymer*, this paper was consequently accepted for publication in *Polymer*.

* Corresponding author.
E-mail address: gert.heinrich@conti.de (G. Heinrich).

PII: S0032-3861(01)00505-5

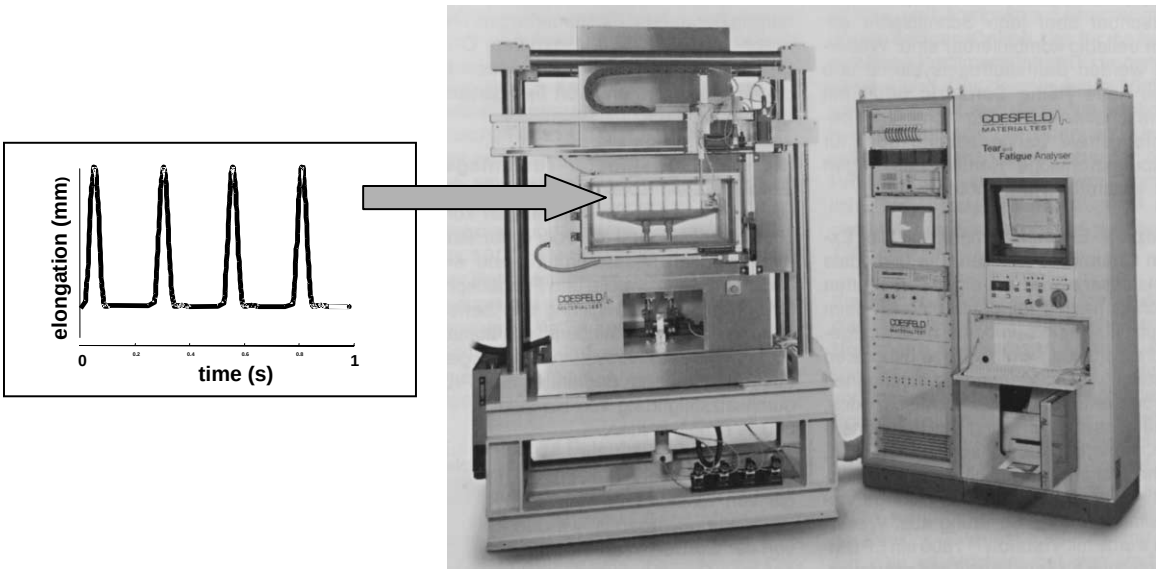

Fig. 1. TFA equipment with load frequency.

Appendix A and Figs. 1 and 2). The material toughness can be characterized as the crack length changes per stress cycle (da/dN) via different stress intensities (this is the procedure that has been selected here!). N being the number of cycles and a being the crack length. It is also possible to characterize toughness with only one fixed exterior load via the current stress, deformation, or energy of specific crack length changes. These are usually parameters of an incipient crack propagation, and a maximum crack propagation before the sample breaks. The implementation of these principal methods is complicated because it has to be ensured that the parameters obtained during the stress test can be directly linked with the stress at the tip of the crack and thus do not, for example, characterize the sample deformation (caused by the specimen configuration). This situation — typical for elastomers — is currently described as follows: "Life prediction of rubber components as an engineering tool is still in the infancy stage. There is a great need for a comprehensive life prediction model which incorporates various approaches [12]."

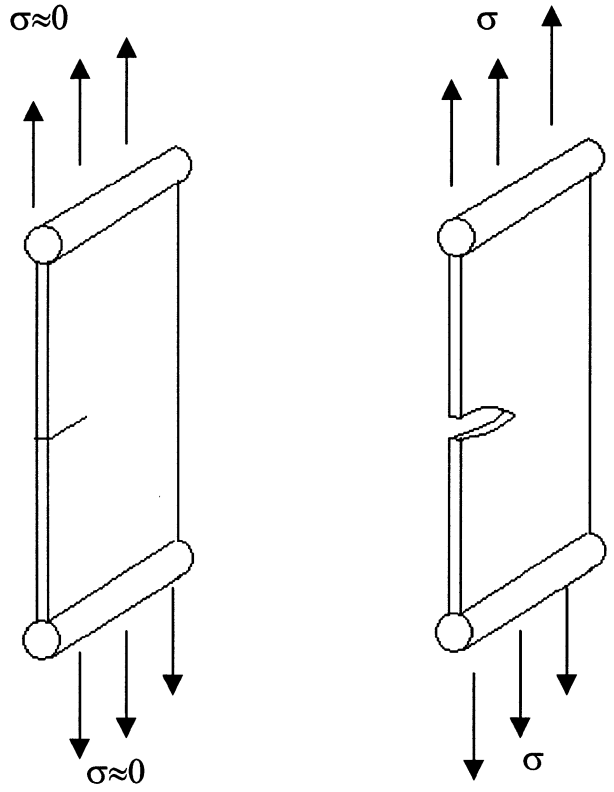

Fig. 2. Geometry of the used rubber samples.

Note that new FEM-supported possibilities for life prediction, in connection with constitutive material laws are available, especially in the case of dynamic stress tests [13]. Here, it is important to understand, and to access at least on a semi-microscopic level, the material behavior occurring directly within the tip of the crack — derived from the macroscopic (in our case non-linear viscoelastic) rubber material. Molecular simulations are successful for amorphous polymeric solid bodies in the glassy state (e.g. Refs. [14–17]).

In this paper, we developed an analytical semi-microscopic model, which combines the assumption of self-similar crack propagation [18,19] with a complex viscoelastic rubber model (standard solid). We present the basic principles and demonstrate the comparison between modeling of dynamic crack propagation and TFA test for the simple case of an unfilled synthetic rubber. The assumption of self-similar crack propagation means that the shape of the deformation zone does not change but becomes self-similar after each cycle, the length s of the zone is increased by the same ratio. After one cycle, the deformation zone is shifted by Δs (Fig. 3).

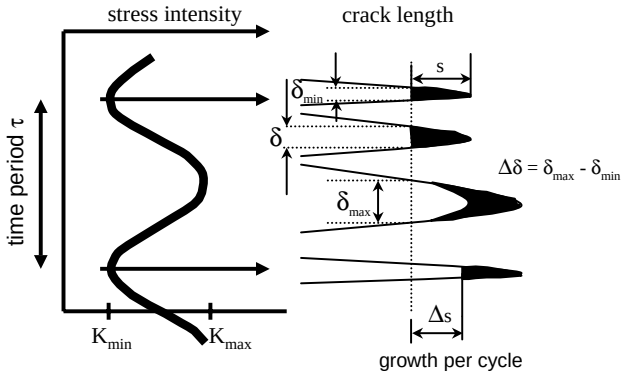

Fig. 3. Crack growth during one cycle according to the model of self-affine crack propagation.

2. Self-similar crack propagation in rubber

We assume that the deformation zone under cyclic stress at the tip of the crack is defined and characterized by a stress intensity factor (see Appendix B) with

$$K_1 = K_{\min}\left(1 + \frac{\Delta K}{K_{\min}} \sin \omega t\right) \tag{1}$$

$$\Delta K = K_{\max} - K_{\min} \tag{2}$$

The true stress σ in the deformation zone at the tip of the crack (Fig. 3) varies as follows, depending on the stress intensity factor K_1:

$$\sigma(t) = \sigma_c \frac{K_{\min}}{K_{1c}}\left(1 + \frac{\Delta K}{K_{\min}} \sin \omega t\right) \rightarrow \sigma(t) = \sigma_0 + \sigma_0 k\, e^{i\omega t} \tag{3}$$

where σ_c is the cohesive stress, K_{1c} the critical stress intensity factor, and

$$\sigma_0 = \sigma_c \frac{K_{\min}}{K_{1c}}; \qquad k = \frac{\Delta K}{K_{\min}} \tag{3a}$$

The stress intensity factor is needed to determine the COD values during the TFA test (see Appendix B). For tension loading, the growth $\Delta\delta$ of the COD δ (*C*rack *O*pening *D*isplacement) after a complete stress cycle is proportional to the deformation rate $d\epsilon/dt$ integrated over a stress period τ [18]:

$$\frac{\Delta\delta}{\delta} = \int_0^\tau \frac{d\epsilon}{dt} dt \rightarrow \frac{\Delta s}{s} \tag{4}$$

with s representing the length of the deformation zone and Δs the crack zone propagation per cycle (Fig. 3).

We assume that the deformation zone continues to creep by $(\Delta s)_{cycle}$ during every cycle. This value corresponds with the known crack length change per cycle, i.e. da/dN (see Appendix B). The latter is thus determined according to Eq. (4) from the elongation rate integrated during a cycle. The following model assumptions are made:

1. Neo Hooke's law is assumed between the nominal stress and deformation according to the theory of rubber elasticity:

$$\sigma = G_i(\lambda - \lambda^{-2}) = G_i \Lambda \tag{5}$$

with G_i the initial shear modulus and $\Lambda = \lambda - \lambda^{-2}$ a non-linear elongation ratio.

2. The temporal change of the crack tip elongation parameter Λ is simulated using a (Eyring) reaction kinetics law for activated viscose materials [20]. Then, we obtain

$$\dot{\Lambda} = A \sinh\left(\frac{v\sigma}{RT}\right) \tag{6}$$

where A is associated with an activation energy, v is an activation volume, and R is the gas constant. According to such characteristics of the stretch parameter Λ, we can introduce a mechanical model with elements as shown in Fig. 4 [20]. The material elements are parts of a standard solid model expanded with a series damper in the secondary creep stage.

Note, the effect of viscous flow on the creep stretch will not occur in the secondary creep stage if one applies the model to the overall viscoelastic behavior of non-damaged rubbers. Then, the dashpot connected in series with the spring can be dropped and the model becomes an equivalent standard solid with three elements, as described in many textbooks.

We obtain the following relations between the stress and stretch parameter, or the time rate of stretch parameter [20]

$$\sigma = \text{const.} \tag{7a}$$

$$\Lambda = \Lambda_i + \Lambda_s + \Lambda_t \tag{7b}$$

and for the temporal change of the elongation parameters

$$\Lambda_i = \frac{\sigma}{G_i} \tag{8a}$$

$$\dot{\Lambda}_s = A_s \sinh(v_s \sigma) \tag{8b}$$

$$\dot{\Lambda}_t = A_t \sinh[v_t(\sigma - G_t \Lambda_t t)] \tag{8c}$$

By integration, the equation for the temporal change of elongation at a given stress (~creep characteristics) is then

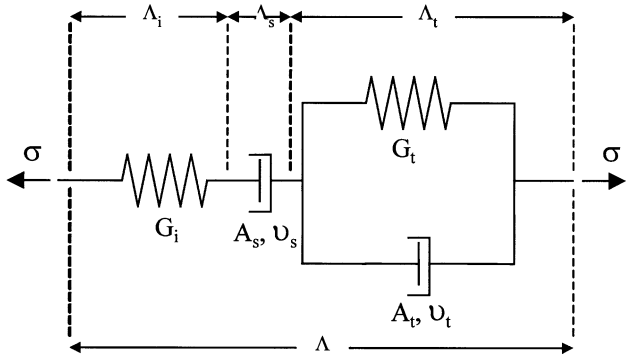

Fig. 4. Schematic diagram of the non-linear mechanical model.

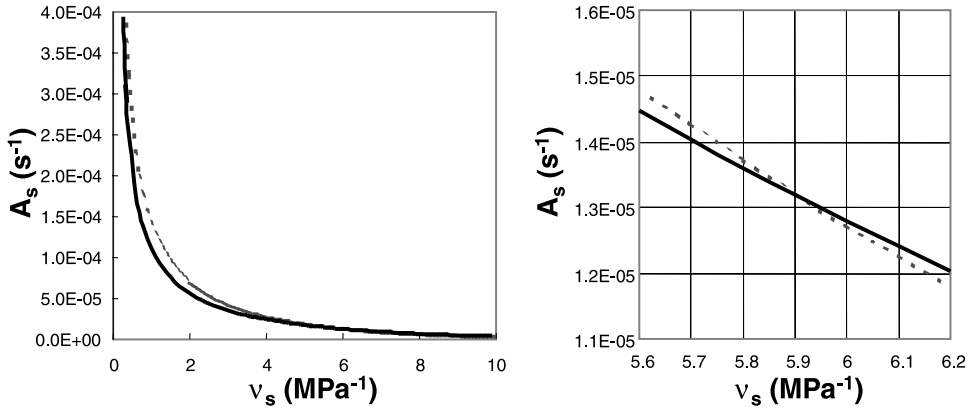

Fig. 5. Estimation of the initial values of material parameters A_s, v_s from stress–strain curves realized at two different strain rates. The procedure is described in the text. (b) A magnification of the cross-point.

as follows (see, for example, Ref. [20]):

$$\Lambda(t) = \frac{\sigma}{G_i} + A_s \sinh(v_s\sigma)t + \frac{\sigma}{G_t}\left\{1 - \frac{2}{v_t\sigma}\tanh^{-1}\left[\tanh\left(\frac{v_t\sigma}{2}\right)\exp(-A_t v_t G_t t)\right]\right\} \tag{9}$$

3. For small elongations, the simplified interconnection between elasticity $\epsilon = \lambda - 1$ (in Eq. (4)) and the elongation parameter applies:

$$\Lambda = \lambda - \lambda^{-2} \approx 3\epsilon + o(\epsilon^2) \approx 3\epsilon \tag{10}$$

4. Elongation ϵ for filled rubber is replaced with the local intrinsic elongation ϵ_{int}, which considers the elongation amplification due to the presence of the filler material carbon black:

$$\epsilon_{int} = X_{eff}\epsilon \tag{11}$$

$$X_{eff} = 1 + 2.5\,\varphi_{eff} + 14.1\,\varphi_{eff}^2 \tag{12}$$

$$\varphi_{eff} = \varphi(1 + 0.5(1 + 0.02139 \times DBP)0.685 - 1) \tag{13}$$

DBP is here the dibutyl phthalate adsorption number characterizing the internal structure (voids) of the filler.

The temporal change of the elongation parameter follows from Eq. (9):

$$\dot{\Lambda}(t) = \frac{d\Lambda(t)}{dt} = A_s \sinh(v_s\sigma) + 2A_t \frac{\tanh\left(\frac{v_t\sigma}{2}\right)e^{-t/\tau_t}}{1 - \tanh^2\left(\frac{v_t\sigma}{2}\right)e^{-2-t/\tau_t}} \tag{14}$$

with $\tau_t^{-1} = A_t v_t G_t$. The parameter τ_t represents a characteristic time of the material that will be discussed later.

The crack propagation according to Eq. (4) follows with the temporal stress Eq. (3) via integration of the intrinsic elongation rate [18]:

$$\frac{\Delta\delta}{\delta} = \frac{X_{eff}}{3}\int_0^\tau \dot{\Lambda}(t)\,dt \rightarrow \frac{(\Delta s)_{cycle}}{s} \tag{15}$$

This integration usually has to be carried out numerically. A simplified model ($\tau_t^{-1} = 0$) yields an analytical solution for the interconnection between the crack growth rate da/dN and the critical stress intensity factor (toughness rate) in the form of the Paris power law [8]. This can be utilized, for example, to simulate very well the dynamic crack propagation in different highly cross-linked polymer networks [18,19].

For elastomeric materials far above glass transition temperature, $v_s\sigma \ll 1$, $v_t\sigma \ll 1$, $\tau_t^{-1} \neq 0$, we obtain according to Eq. (15) together with Eqs. (3), (11)–(14) the following result:

$$\frac{(\Delta s)_{cycle}}{s} = X_{eff}\frac{\sigma_0}{G_t}\left\{\frac{\tau}{\tau_s} + (1 - e^{-\pi/\tau_t}) + \frac{2\pi k\tau}{\tau_t}\left[\frac{(1 - e^{-\pi/\tau_t})}{(\tau^2/\tau_t^2) + 4\pi^2}\right]\right\} \tag{16}$$

where the time τ_s is related to the model parameters of the flow enhanced standard solid as follows: $\tau_s^{-1} = A_s v_s G_t$. Eq. (16) shows that the model parameters appear in the two characteristic material times τ_s and τ_t that will be discussed in Section 4. In the following example, we consider unfilled polymer materials and discard elongation amplification by fillers. Investigations with filled rubbers will be published in a separate paper.

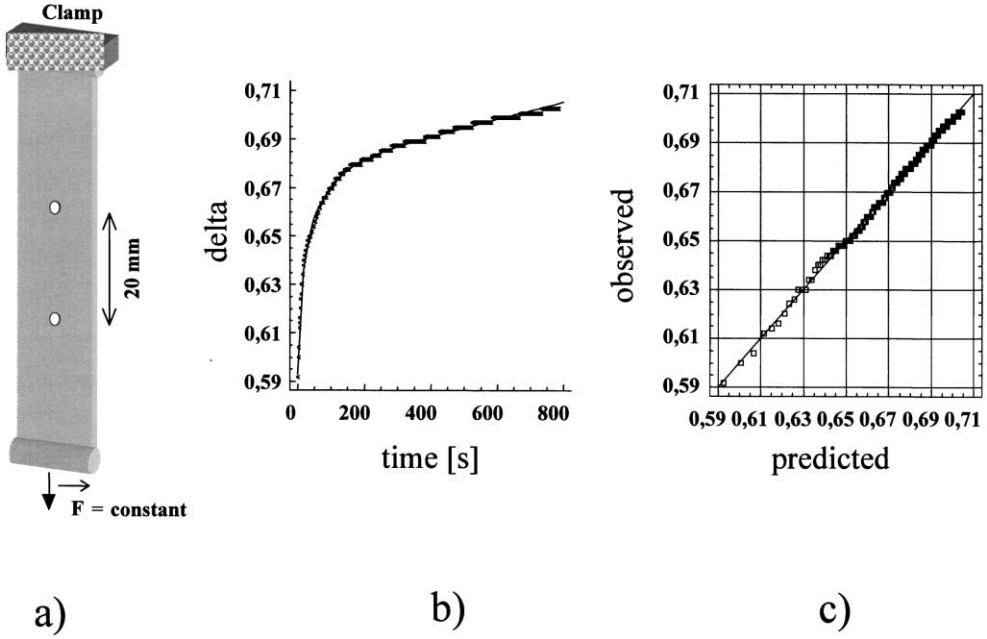

Fig. 6. Estimation of the parameters of Eq. (9) according to a non-linear regression using data of the stress–time curve (b) recorded on samples shown in (a). The quality of regression is shown in (c).

3. Determining parameters

Step 1: Determining the initial values A_s, v_s:

In case of two different constant elongation rates, the stress–strain curves of the two experiments are estimated. The following applies to $A_t = 0: \dot{\Lambda} = \text{const} = A_s \sinh(v_s \sigma)$. This yields the two functions $A_s = f(v_s)$. The intersecting point determines the initial values for the material parameters A_s, v_s (Fig. 5).

Step 2: A non-linear regression determines the parameter of an elongation–time curve (Eq. (9)) with elongation under constant stress (Fig. 6).

Table 1 depicts an example of the parameters for an unfilled rubber consisting of styrene butadiene copolymer SBR 1500 and cross-linked with 1.2 phr (= parts of weight per hundred parts of polymer) of sulfur and 1.2 phr *N*-cyclohexylbenzothiazole-2-sulfenamide (CBS) accelerator. Although, we have presented here the derivation of the general theory of dynamic crack propagating in filled rubbers, we restrict the example to the simplest case of an unfilled sample. The corresponding results of a larger set of samples (including filled rubbers) will be published in a separate paper.

The quality of the regression is shown in Fig. 6c, comparing the curve values calculated with the parameters given in the measured curve.

Table 1

G_i (MPa)	A_s (s^{-1})	v_s (MPa^{-1})	G_t (MPa)	A_t (s^{-1})	v_t (MPa^{-1})
0.625	1.31×10^{-5}	6.03	3.43	2.4×10^{-4}	14.5

The comparison between the crack propagation rate determined from Eq. (16) and the TFA results is depicted in Fig. 7 where the crack propagation rate is shown as a function of the stress intensity maximum.

The critical stress intensity factor K_{1c} in Eq. (16) was determined with a notched sample using a static tensile test. It characterizes the toughness at maximum crack length before the sample breaks. The cohesive stress σ_c was determined from the Young modulus E of a tensile–compression test (non-notched sample) according to $\sigma_c \approx E/15$ [11,21].

4. Conclusions and final remarks

We have shown that the dynamic crack propagation in rubbers can be modeled via the combination of three physical concepts: (i) self-affine crack propagation, (ii) stress intensity factor (crack tip opening displacement), and (iii) Eyring-like flow-enhanced neo-Hookean standard solid as a representative of the rubber solid. The effect of viscous flow on the creep stretch will not occur in the second creep stage if one removes the dashpot connected in series with the spring. Then, the (linear standard solid) model describes only the viscoelastic behavior of a non-damaged rubber sample. New intrinsic material parameters (v_s, v_t, A_s, A_t) are introduced which can be estimated from simple (non-destructing) stress–strain and creep experiments. These parameters are related to activation volumes and activation energies, respectively, at the crack tip material which is described with the generalized standard solid model. A reasonable interpretation follows from the inverse parameters $1/v_{s,t}$ [MPa], $1/A_{s,t}$ [s] having the meaning of intrinsic

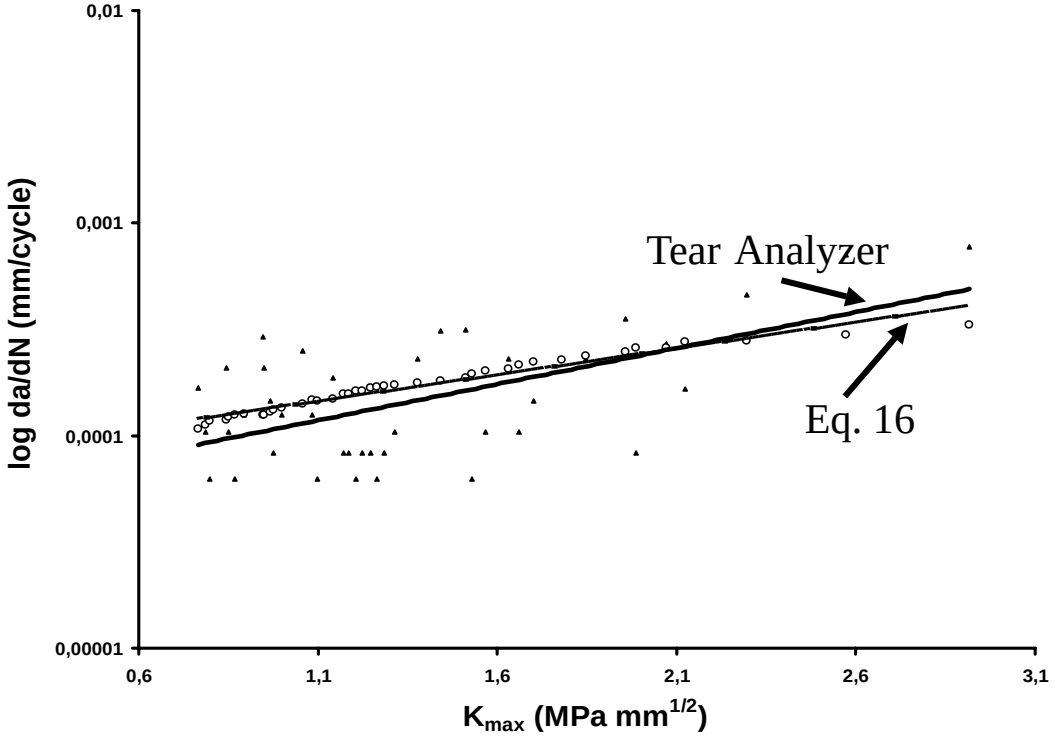

Fig. 7. Comparison between the crack propagation rate determined from Eq. (16) and the TFA results. The crack propagation rate is shown as a function of the stress intensity maximum. The used sample is an unfilled SBR rubber.

moduli and times, respectively. The combinations $\tau_s^{-1} = A_s v_s G_t$ and $\tau_t^{-1} = A_t v_t G_t$ define the two characteristic relaxation times of the rubber material ($\tau_s \approx 10^3$ s, $\tau_t \approx 10^2$ s). Both times are much larger than the stress period $\tau = 1/30$ s. In this case $\tau/\tau_{s,t} \ll 1$ only the third term in Eq. (16) yields significant contributions to the crack length propagation. The first two terms are not dependent on the stress intensity and determine the transition to the low (zero) stress intensity amplitude region which is not involved within our model considerations. Otherwise, the dependence of crack propagation on stress intensity amplitude is mainly determined using the third term in Eq. (16). For a fixed stress intensity, $k = \Delta K/K_{min}$ reaches its maximum for $\tau = \tau_c \approx 6.4\tau_t$. We find $\tau_c \approx 640$ s for our example. This time τ_c corresponds to a critical frequency of the stress intensity, say $\omega_c = 2\pi/\tau_c$ ($\sim 10^{-2}$ s^{-1}), where crack propagation reaches a maximum for given stress intensity conditions. In the case of load frequencies $\omega > \omega_c$, the material behaves 'stiffer' and less sensitive against crack propagation. In the opposite case, $\omega < \omega_c$, the material approaches the static case where again the dynamic crack propagation rate decreases. For $\omega = \omega_c$, a calculation of the maximum possible crack propagation per cycle yields a value of $v_{(crack)crit} \sim 10^{-3}$ m/cycle which is high above the experimental estimated value for the used loading frequency 30/4 Hz, $v_{crack} \sim 10^{-7}$ m/cycle (see Fig. 7).

The purpose of this paper is to offer some new insights to the problem of dynamic crack propagation in rubbers. Moreover, findings such as critical frequencies can be used for guidelines in predictive testing of rubber materials. However, we have not given any molecular interpretations of the two relaxation times that were introduced. We speculate that the large values of the relaxation times (10^2, 10^3 s) can be traced back to the extremely long-time relaxation behavior of free dangling ends [22] that arise during crack propagation and the cutting of network chain.

We note that our approach and Eq. (4) is restricted to tensile deformation. The neo-Hooke's law (Eq. (5)) leads to further restriction of the approach to amorphous rubbers and excludes strain-crystallizing rubber materials.

We finally conclude that dynamic fracture and fatigue of rubbery materials are complex phenomena. However, certain physical concepts can be used to predict the crack propagation properties, since failure of rubbers is preceded by viscoelastic responses.

Acknowledgements

The authors thank Continental AG for permission to publish the paper.

Appendix A

The TFA measurement (Fig. 1) was carried out with a controlled elongation of 22.5%.

The following data were recorded and analyzed:

- cycle number, N
- min. force
- max. force
- max. tension
- overall energy density, W_{tot}
- elastic energy density, W_{el}
- true elongation, ϵ
- crack length, a

The (pulsed) stress frequency amounted to 30/4 Hz.

Appendix B

Using the critical stress intensity factor K, we introduce a one-parameter description of the stress field surrounding a crack tip, generally under the condition of linear elastic materials with small plastic deformations. It is possible to define a critical stress intensity factor according to Refs. [11,21] for polymer systems with samples notched on one side:

$$K = Q\sigma a^{1/2}$$

with a representing the crack length, σ the current stress, and Q a geometry factor

$$Q = \left[1.99 - 0.4\left(\frac{a}{w}\right) + 18.70\left(\frac{a}{w}\right)^2 - 38.48\left(\frac{a}{w}\right)^3 + 53.85\left(\frac{a}{w}\right)^4 \right]$$

where w is the sample width.

We use K_1 (see Eq. (1)) to determine the COD values at any time during a TFA test:

$$\mathrm{COD} = \frac{8K_1}{E}\frac{\sqrt{a}}{\sqrt{2\pi}}$$

References

[1] Gent AN. In: Eirich FR, editor. Strength of elastomers, Science and technology of rubber. New York: Academic Press, 1978.
[2] Fukahori Y. Int Polym Sci Technol 1998;25:T/50.
[3] Gerber G, Struve J. Kautsch Gummi Kunststoffe 1999;52:400.
[4] Grellmann W, Cäsar T, Heinrich G. Kautsch Gummi Kunststoffe 1999;52:37.
[5] Böhm D, Struve J. Tire Technol Int 2000:55–58.
[6] Reincke K., Luch R., Gnellmann W., Heinrich G. Rubb Chem Technol. In press.
[7] Grellmann W, Reincke K, Lach R, Heinrich G. Kautsch Gummi Kunststoffe 2001, in press.
[8] Seldén R. Prog Rubb Plast Technol 1995;11:1.
[9] Lake GJ. Rubb Chem Technol 1996;68:435.
[10] Ishimaru S. Int Polym Sci Technol 1998;25:T/58.
[11] Kinloch AJ, Jung RJ. Fracture behaviour of polymers. London: Applied Science Publishers, 1983.
[12] Pannikottu A. Rubber Asia 1998;12:131.
[13] Struve J, Heinrich G, Gerber G. In preparation.
[14] Chakrabarti BK, Benguigui LG. Statistical physics of fracture and breakdown in disordered systems. Oxford: Clarendon Press, 1997.
[15] Kramer EJ. Plast Rubb Compos Process Appl 1997;26:241.
[16] Persson BNJ. J Chem Phys 1999;110:9713.
[17] Persson BNJ. Phys Rev Lett 1998;81:3439.
[18] Fischer M, Martin D, Pasquier M. Macromol Symp 1995;93:325.
[19] Fischer M. Adv Polym Sci 1992;100:313.
[20] So H, Chen UD. Property modeling of viscoelastic elastomers. In: Cheremisinoff NP, editor. Elastomer technology handbook. Boca Raton: CRC Press, 1993.
[21] Brostow W, Corneliusen RD. Failure of plastics. München, Wien: Hanser Publisher, 1986.
[22] de Gennes PG. Scaling concepts in polymer physics. Ithaca, New York: Cornell University Press, 1979.